

Diverse Stability and Catalytic Properties of Human Tryptase α and β Isoforms are Mediated by Residue Differences at the S1 Pocket[†]

Trevor Selwood,^{*,§} Zhi-Mei Wang,[‡] Darrell R. McCaslin,[#] and Norman M. Schechter^{§,¶}

Department of Dermatology, Department of Medicine and Department of Biochemistry and Biophysics, University of Pennsylvania, Philadelphia, Pennsylvania 19104 and Department of Biochemistry, University of Wisconsin, Madison, Wisconsin 53706

Received August 8, 2001; Revised Manuscript Received December 17, 2001

ABSTRACT: Recombinant human tryptases (rHTs) corresponding to α and β isoforms were characterized. rHT β was similar to tryptase isolated from skin (HST); it was a tetramer, hydrolyzed model substrates efficiently, and was functionally unstable when incubated under physiological conditions. Activity was lost rapidly ($t_{1/2} \approx 1$ min) by a reversible process similar to that observed for the spontaneous inactivation of HST. Circular dichroism (CD) and intrinsic fluorescence emission (IFE) spectra of active rHT β corresponded to those of active HST and upon spontaneous inactivation IFE decreased in parallel to activity loss. rHT α differed from HST in catalytic ability and stability. rHT α did not react with model substrates, an active site titrant, or a competitive inhibitor of HST/rHT β . IFE and CD spectra were similar to those of the active and not the spontaneously inactivated form of HST. Under physiological conditions, rHT α IFE decreased at a rate 900-fold slower than that observed for HST, and rHT α remained tetrameric when examined by size exclusion chromatography at physiological salt concentration. Thus, rHT α is a stable “inactive” form of HT. Three active site variants of rHT α , K192Q, D216G, and K192Q–D216G were characterized. Residues 192 and 216 (chymotrypsinogen numbers for residues 191 and 215 of rHT α) lie at the entrance to the primary specificity (S1) pocket, and the mutations converted them to the residues of HT β . While K192Q displayed the same properties as rHT α , the catalytic and stability characteristics of D216G and K192Q–D216G progressively approached those of HST. Thus, the contrasting stability/activity properties of rHT α and rHT β are largely related to differences at the S1 pocket. On the basis of the properties of the variants, we suggest that the side chain of Asp216 is blocking and stabilizing the S1 pocket and that this stabilization is sufficient to prevent spontaneous inactivation.

Tryptases are serine proteases found in mast cells (1) that, as the name implies, have a substrate specificity similar to that of bovine trypsin (2–4). HT¹ isolated from skin and lung is distinguished from most other serine proteases by its tetrameric structure and functional instability (5–8). Functional instability is the loss of HT enzymatic activity through a nonproteolytic process that we and others have termed spontaneous inactivation. Under physiological conditions, enzymatic activity is lost with a $t_{1/2}$ of 1 min. The rate

of activity loss is sensitive to temperature, pH, and salt concentration, and is dramatically reduced by the binding of sulfated polysaccharides (5, 6, 9). Although the mechanism and biological significance of spontaneous inactivation is controversial (5, 10–13), most laboratories agree with our original findings that the process can be reversed by the addition of heparin to inactivated HT and that it is the result of reversible and limited structural changes (6, 11, 14).

We have provided evidence that spontaneous inactivation is the reversible conversion of HT to a zymogen-like form and that dissociation of the tetramer is produced by this conversion (11, 14). The zymogen conformation of a serine protease is typically associated with the incomplete formation of the S1 subsite, or primary specificity pocket, due to the absence of an ionic bond between the α -amino group of Ile16² and the carboxyl group of Asp194 (15). Alternatively, it has been proposed that spontaneous inactivation is initiated by tetramer dissociation, i.e., the HT tetramer is inherently weak and readily dissociates to inactive subunits in the absence of heparin (12, 13, 16). The crystal structure of HLT revealed a frame-like tetramer with two different size interfaces, each formed by loops structurally unique to HT (8). Both interfaces are located near the active site, which

[†] This work was supported by NIH Grant AI45075.

* Corresponding author: Trevor Selwood, Department of Dermatology, University of Pennsylvania, Clinical Research Building/Rm 240, 415 Curie Blvd., Philadelphia, PA, 19104. Tel: 215-898-0168, fax: 215-573-2033, e-mail: selwood@mail.med.upenn.edu.

[§] University of Pennsylvania, Department of Dermatology.

[¶] University of Pennsylvania, Department of Biochemistry and Biophysics.

[‡] University of Pennsylvania, Department of Medicine.

[#] University of Wisconsin, Department of Biochemistry, Biophysics Instrument Facility.

¹ Abbreviations: AEBSF, 4-(2-aminoethyl)benzenesulfonyl fluoride; APPA, 4-amidinophenylpyruvic acid; CBZ, *N*-carbobenzoxy; CD, circular dichroism; EK, enterokinase; EKCS, enterokinase cleavage site; HT, human tryptase; HST, human skin tryptase; HLT, human lung tryptase; IFE, intrinsic fluorescence emission; L-BAPNA, *N* α -benzoyl-L-arginine-pNA; MUGB, 4-methylumbelliferyl 4-guanadinobenzoate; NA, 4-nitroanilide; pAb, *p*-aminobenzamide; rHT, recombinant human tryptase; SD, standard deviation; SEC, size exclusion chromatography.

² Residues of serine proteases are referred to using numbering based on alignment with bovine chymotrypsinogen. The alignment for rHT is that described by Pereira (8).

was apparently stabilized by the binding of an inhibitor. Instability of the smaller interface has been suggested as the cause for tetramer dissociation and activity loss (13, 16).

Analysis of specific gene products, instead of possible mixtures isolated from tissues, may help to define and understand further the unusual properties of HT. HT genes fall into two closely related groups termed HT α and HT β . Six genes/alleles have been identified within these groups, HT α .I (17, 18), HT α .II (19), HT β .Ia, HT β .Ib (19–21), HT β .II, and HT β .III (21). In addition, a separate gene encoding for a transmembrane form of HT (termed TMT or HT γ) has been described (22, 23). The published sequences of the HT α s differ from those of the HT β s by 14–18 amino acids depending on the pairing. On the basis of the crystal structure of HLT, 6–9 of these differences lie at subunit interfaces and 1–2 lie at the S1 pocket (8).

Several laboratories including ours have produced rHT β (24–28). Initial characterizations of rHT β described structural and catalytic properties similar to those of HST and HLT. Characterization of rHT α has been more controversial. While one study has indicated that proHT α cannot be processed to its mature form within the cell (9), another study found that rHT α produced in COS cells was able to activate a trypsin-sensitive cellular receptor (29). Huang et al. (25) have produced a mature rHT α in baculovirus using a pseudozymogen construct. Mature rHT α demonstrated highly reduced catalytic activity as compared to rHT β . An Asp instead of a Gly residue at position 216 within the active site was identified as an important factor affecting the catalytic activity. None of these studies have characterized rHT α with respect to structural integrity and spontaneous inactivation.

In this study, the structure, functional stability, and catalytic efficiency of rHT α .I was compared to rHT β .II. rHT β and rHT α isoforms were found to exhibit diametrically opposed properties. Whereas rHT β was enzymatically active but structurally unstable, rHT α was enzymatically inactive, at least with substrates hydrolyzed efficiently by HST/rHT β , but structurally stable. On the basis of analysis of three rHT α variants, these contrasting properties are largely accounted for by residues forming the S1 pocket and not by those at subunit interfaces. These results indicate that the structure of the S1 subsite of HT is central not only to catalysis but also to spontaneous inactivation and the integrity of the tetramer structure.

EXPERIMENTAL PROCEDURES

Materials. Bovine intestinal mucosal heparin, 5 kDa average mass, was from Calbiochem. Substrates and porcine EK (catalog number E0885) were from Sigma. Heparin-Sepharose and the Superose 12HR 10/30 FPLC column were from Pharmacia. The vector pAcGP67B was obtained from Pharmingen. Ultrafiltration membranes were from Millipore and Gel Code Blue was from Pierce.

Production of rHT-Fusion Proteins. DNA sequences coding for mature rHT α .I and rHT β .II were produced from genomic DNA by exon copying and coupling (28, 30). The primer sequences used to amplify the regions of the four exons (II–V) encoding mature HT β .II were previously reported (28). These primers also amplified HT α .I exons II, III, and V. To produce HT α .I exon IV, a new pair of primers

was produced reflecting the difference in amino acid sequence between HT α .I and rHT β .II (P150R, T186S, R187Q, and Q192K). Because of our overlap strategy, the sequence difference also required the production of a new sense primer coding for the end of exon IV and the beginning of exon V. The sequence of the sense/antisense primers used for the amplification of exons IV and V were the following: exon IV: 5'CGATGTGGACAATGATGAGCCCCTCCCACCG-CCA3' and 5'CTTGCAGGAGTCCCTCTGGC3', and exon V: 5'AGAGGGACTCCTGCAAGGGCGACTCTGGAGGG-CC3' and 5'CCG(GAATTC)TCACGGCTTTTGGGGAC3'. Within the parentheses is an *EcoRI* restriction site.

The exon products coding for HT α were coupled together in the appropriate order using the overlap-extension PCR method of Horton et al. (31). The nucleotide sequence for the EKCS was added to the N-terminus of rHT α .I DNA using a primer coding for the EKCS and the N-terminus. To produce the fusion protein DNA, EKCS-HT DNA was cloned into a pAcGP67B vector immediately downstream of the bovine ubiquitin DNA sequence. The ubiquitin DNA was previously placed in the vector downstream of the GP67 signal sequence and the polyhedrin promoter. The vector was cotransfected with BaculoGold DNA into Sf9 cells and propagated. The fusion protein was expressed in Hi-5 cells. To produce rHT variants, DNAs coding for rHT α or rHT β were mutated by the PCR method of Ho et al. (32). Sequences of all rHTs were confirmed by DNA sequencing.

Purification of HST and rHTs. HST was purified as previously described (11). rHTs were purified by the following method with all steps at 25 °C, except for the ammonium sulfate precipitation step at 4 °C. Medium (typically 1 L) obtained after 72 h of expression was diluted with an equal volume of 20 mM MES, pH 5.5, and immediately applied to a 100-mL heparin-Sepharose column equilibrated in 20 mM MES, pH 5.5. The acidic pH and reduced salt concentration resulted in increased adsorption of the fusion protein to the resin. The column was washed with 800 mL of a solution of 50 mM NaCl, 0.01 M MOPS, pH 6.8. All subsequent solutions utilized in purification steps were buffered at pH 6.8 using 0.01 M MOPS. The fusion protein was eluted with a single step of 0.5 M NaCl. Fusion protein fractionation was monitored by assay of EK-activated aliquots removed from fractions and/or by SDS-PAGE. Fractions containing the fusion protein were combined, and ammonium sulfate was added to 85% saturation. After 1 h at 4 °C, the precipitate containing fusion protein was collected by sedimentation at 30 000 rpm (100 000 g) for 30 min in a Ti45 rotor. The resulting precipitate was resuspended in 10 mL of 0.2 M NaCl and clarified by centrifugation at 12 000 rpm (17 000 g) for 10 min in a SS-34 rotor. No HT activity was detected in the fusion protein preparations. To produce mature rHTs, heparin (50 mg/mL stock) to a final concentration of 0.5 mg/mL and EK to a final concentration of 10 Sigma units/mL were added to fusion protein solubilized in 5–10 mL of 0.2 M NaCl. After a 1–2 day incubation, the processed material was diluted 10-fold with buffer and applied to a 10-mL heparin-Sepharose column. The column was developed with a 150-mL linear gradient from 0.2 to 1 M NaCl. All rHTs eluted as a symmetrical peak near 0.7 M NaCl. Fractions containing rHT were pooled, and solid NaCl was added to produce a

final concentration of 2.0 M. The pool was concentrated by ultrafiltration using a PM10 membrane. The final concentration of rHTs was between 30 and 60 μ M. The concentrated solution was aliquoted, frozen by immersion in liquid nitrogen, and stored at -70 °C until needed.

Estimation of Enzyme Concentration. The concentrations reported are for HT subunits. Subunit concentration was based on $A_{280\text{ nm}}$ assuming the same extinction coefficient for all rHTs. This extinction coefficient was calculated to be $64\,900\text{ M}^{-1}\text{ cm}^{-1}$ assuming 9 Trp, 10 Tyr, and 4 cystine residues per subunit (33). $A_{280\text{ nm}}$ of rHTs in 8 M GuHCl and in buffer were similar, supporting the applicability of the calculated value. Subunit concentrations estimated from $A_{280\text{ nm}}$ measurements were related to hydrolytic rates to obtain molar specific activities. For enzymatically active rHTs, subunit concentration also was determined by burst titration with MUGB (34).

Enzymatic Assays. Standard assay conditions were 0.2 M NaCl, 0.1 M Tris-HCl, pH 8.0, 0.1 mg/mL heparin, 9% Me₂SO, 25 °C plus substrate. Heparin was included to prevent activity loss via spontaneous inactivation during the assay period. Inclusion of heparin in assays is a departure from previous studies (6, 11, 14) but was necessary because of the more rapid inactivation rates of the rHT β s. Despite the inclusion of heparin, assay conditions will not rescue HT inactivated by spontaneous inactivation (see next section). To obtain initial rates, product formation typically was monitored continuously for 3 min periods at 410 nm using a Beckman DU 640 spectrophotometer. Product formation was linear and less than 10% of the substrate was consumed.

$k_{\text{cat}}/K_{\text{m}}$ values were determined under pseudo first-order conditions. For all substrates, $[S]_0 = 0.05\text{ mM}$, which was well below the K_{m} , estimated to be above 0.8 mM for all substrates. Progress curves were fit using a single-exponential function to obtain k_{obs} , the pseudo first-order rate constant for the process; $k_{\text{obs}}/[E]$ was used to obtain $k_{\text{cat}}/K_{\text{m}}$. Because of the limited solubility of substrates, plots of initial rate vs $[S]_0$ were not adequate to determine individual kinetic parameters k_{cat} and K_{m} . Under our assay conditions, substrates were found to precipitate at the following concentrations: L-BAPNA, 3 mM; CBZ-GPR-NA, 1 mM; tosyl-GPK-NA, 2 mM; tosyl-GPR-NA, 0.8 mM.

Spontaneous Inactivation and Reactivation. Spontaneous inactivation was initiated by dilution of stock rHT or HST (stabilized at 4 °C in 2.0 M NaCl) to inactivation conditions of 0.2 M NaCl, 0.01 M MOPS, pH 6.8, and indicated temperature. Controls were the same magnitude of dilution into stabilizing solutions of either 2.0 M NaCl or 0.2 M NaCl, 0.5 mg/mL heparin in 0.01 M MOPS, pH 6.8, and indicated temperature. They were initiated at the time of the decay, and the 0-time point of the control was used to convert decay/reactivation data to fractional activity. Like HST (11), estimates of initial rHT control activity were in proportion to the dilution indicating that little if any rHT activity was lost as a result of dilution itself. For reactivation of rHTs, the sample was allowed to decay to less than 5% activity. At this time, it was equilibrated to 25 °C for 10 min, and then heparin was added. Rates were adjusted to account for a 10% dilution of the enzyme due to heparin addition.

To measure activity during decays and reactivations, small aliquots were removed from the incubation mixtures and diluted 25–500-fold into assay media containing either 1

mM L-BAPNA or tosyl-GPK-NA depending on the rHT and the protease concentration being evaluated. The aliquot volume removed from the decay/reactivation for activity measurement was equivalent to that needed to produce an activity of 0.10 $\Delta A_{410\text{ nm}}/\text{min}$ by the 0 time control. The low HT concentration (2–35 nM) in the assay resulting from the dilution precludes reactivation of HT by heparin in the assay media (6). The reliability of inactivation rates determined by monitoring activity is supported by their correspondence to rates of IFE loss shown in Table 2.

Physical Measurements. SEC was performed using a Superose-12HR 10/30 FPLC column equilibrated at 25 °C in 2.0 or 0.2 M NaCl, 0.01 M MOPS, pH 6.8. 0.25 mL samples were loaded, the flow rate was 0.5 mL/min, and approximately 40 min was required for each analysis. $A_{280\text{ nm}}$ and $A_{230\text{ nm}}$ was continuously monitored using an in-line PE LC-235 diode array detector. Fractions of 0.5 mL were collected so that enzymatic activity could be monitored.

SDS–PAGE of rHTs was performed by discontinuous gel electrophoresis. The running gel consisted of 15% acrylamide/0.4% bis-acrylamide (35). Samples were denatured by heating at 90 °C for 10 min in sample buffer containing 1% SDS and 15 mM dithiothreitol. Visualization was achieved by staining with Gel Code Blue as described by the manufacturer.

CD spectra were recorded on an AVIV Instruments, Inc. model 202SF CD spectrophotometer in a 0.1 cm path length cuvette at 25 °C. Data were recorded at 1 nm intervals and averaged for 10 s for rHT α and 3 s for all other rHTs. The concentration of rHT was determined from an absorbance spectrum in the same cuvette measured on a Cary 400 Bio UV/Visible spectrophotometer. The concentrations were 6.5, 12.5, and 12.5 μ M for rHT α , rHT α -D216G, and rHT β -E149T, respectively. After subtraction of a solvent baseline, the concentration and a mean residue weight of 112 were used to convert the CD spectra to molar ellipticity.

Sedimentation equilibrium of rHT-D216G was performed in a Beckman Optima XLA analytical ultracentrifuge. Initial protein concentrations in three independent runs were 9, 5.6, and 2.4 μ M in 2 M NaCl, and 0.01 M MOPS, pH 6.8. The density of the solvent was 1.084882 g/mL as determined by an Anton-Paar DMA 5000 density meter; the partial specific volume of rHT-D216G was calculated as 0.736 mL/g. Measurements were made at 4 °C at speeds ranging from 8 700–20 000 rpm. Equilibrium was ascertained as superimposable gradients recorded several hours apart. In some instances, the equilibrium gradient was monitored for about 10 h with no discernible changes, demonstrating a lack of dissociation or aggregation on the time scale of the equilibrium experiment. Final protein concentrations at equilibrium ranged from zero to about 30 μ M.

Fluorescence experiments were performed using a Photon Technology International QM-C60 fluorescence spectrophotometer in photon counting mode. The cell holder was thermostated by a circulating water bath. Excitation was at 295 nm, and IFE spectra were recorded from 305 to 405 nm at a rate of 4 nm/s and at 1 nm intervals. Excitation and emission slits were set to give a 4 nm bandpass, and the cuvette had a path length of 1 cm. Background spectra of buffer were subtracted from all HT spectra to correct for the Raman peak at 327 nm. Data at 330 nm reported in time-

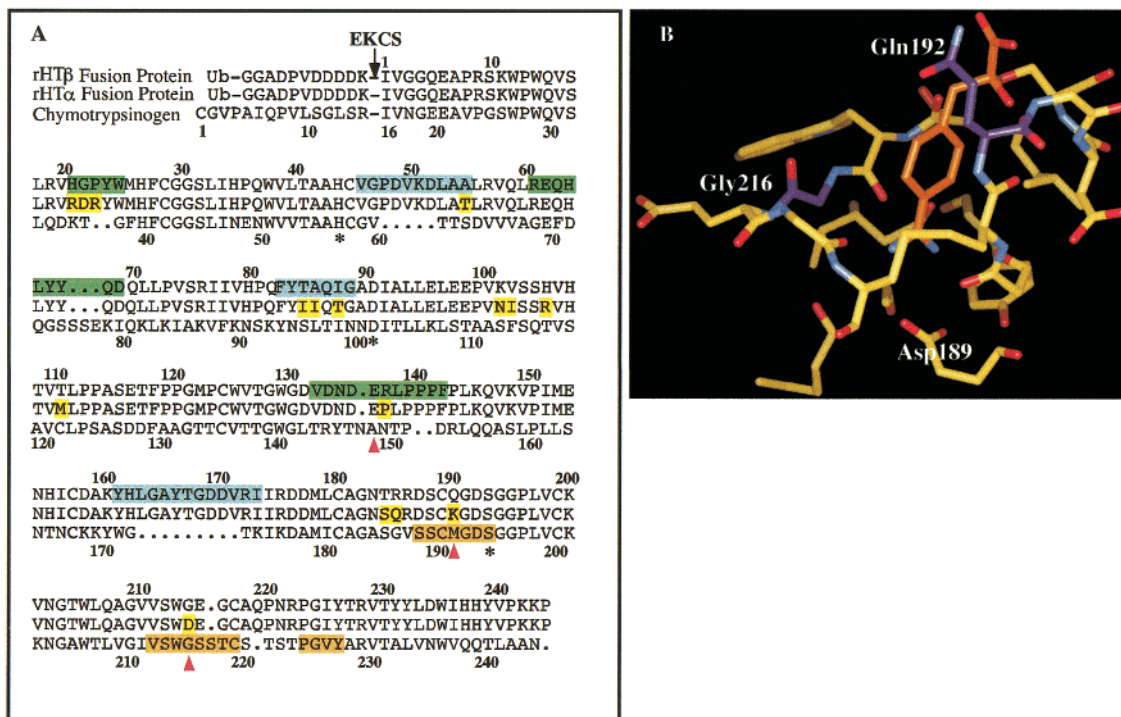


FIGURE 1: The amino acid sequences of rHT α and rHT β fusion proteins (A) and structure of the S1 pocket (B). In panel A, numbering above the sequences marks the linear amino acid sequence of HT, while the numbering below is based on alignment to chymotrypsinogen A as described by Pereira et al. (8). Insertion and deletions between HT and chymotrypsinogen A are indicated by spaces with dots. Highlighted in green and blue are the loops forming the small and large interfaces, respectively, of the HT tetramer. Although not labeled in the figure, the loops comprising the small interfaces have been referred to as the 37, 70–80, and 152 loops, and those comprising the large interfaces are referred to as the 60, 97, and 173 loops (8). Highlighted in orange are the residues that form the primary specificity (S1) pocket. Highlighted in yellow in the rHT α sequence are the 16 residues that differ from those at homologous positions of rHT β . Red triangles denote the positions (149 of rHT β and 216 of rHT α) that were mutated to produce variants. Asterisks indicate the residues of the catalytic triad. EKCS denotes the EK cleavage site, Ub is bovine ubiquitin. In panel B, the structure of the S1 pocket of rHT β is shown to highlight the location of Gln192 and Gly216 (chymotrypsinogen numbering). Both residues are colored purple and are located at the rim of the S1 pocket. The covalently bound inhibitor APPA (colored orange) is protruding toward Asp189 at the base of the pocket. Oxygens and nitrogens are in CPK colors. The coordinates were obtained from the Brookhaven Protein Data Bank; accession number 1AOL (8). The structure was visualized using WebLab ViewerLite by Molecular Simulations Inc.

course studies were obtained from IFE spectra taken at indicated times. An automatic shutter was employed in time-course studies to limit irradiation of the sample to data collection periods.

The fluorescence enhancement of pAb upon binding to HTs was monitored as previously described (11). Emission spectra (2 nm bandpass) were recorded between 340 and 440 nm with 325 nm excitation (2 nm bandpass), and background spectra were subtracted to remove the Raman peak at 365 nm. Spectra of 40 μ M pAb in the absence and presence of 2.1 μ M rHT α or 2.7 μ M rHT β -E149T were obtained. Measurements were made at 25 $^{\circ}$ C in a 1 cm path length cuvette containing a 1 mL solution of 0.2 M NaCl, 0.01 M MOPS, pH 6.8, and 0.5 mg/mL heparin.

Data Analysis. Linear and nonlinear least-squares curve fittings to the data were performed within the Igor Pro data analysis package by Wavemetrics, Inc. Error estimates reported in the text are ± 1 SD from the mean. Sedimentation equilibrium analyses which included global fitting of all data sets to various models were performed using software written by author D.R.M. within the Igor Pro environment.

RESULTS

Expression and Sequence of rHTs. rHT fusion proteins were expressed in baculovirus infected insect cells. The fusion protein construct and the deduced amino acid se-

quences of rHT α and rHT β characterized in this study are shown in Figure 1A. The sequence of rHT β was identical to that of HT β .II except for an Ile instead of a Val at position 176. Ile is residue 176 in both of the natural HT α isoforms. The sequence of rHT α was identical to rHT α .I, except that residue 59 was a Val instead of a Leu. This variation was due to the primer sequence used to amplify exon II. The primer was based on the genomic sequence of HT β .II which codes for Val at position 59. Both substitutions are highly conservative replacements. As a result of the two substitutions, the rHTs in Figure 1A differ by 16 residues instead of the 18 residues predicted from sequences reported in the literature (20, 21).

In addition to the above rHTs, three variants of rHT α (D216G, K192Q, and K192Q–D216G) and one variant of rHT β (E149T) also were produced. The variants of rHT α converted the indicated residues to those found in rHT β . On the basis of the crystal structure of HLT (HT β .II), these residues would lie relatively close to each other at the rim of the primary specificity (S1) pocket (Figure 1B). rHT β -E149T was produced to eliminate a cleavage/inactivation site sensitive to EK within the enzyme portion of the fusion protein. Cleavage of rHT β into two bands of approximately half the mass of the intact protease was noticed while using SDS–PAGE to monitor the course of activation by EK (28). Amino acid sequencing of these bands identified Arg150–

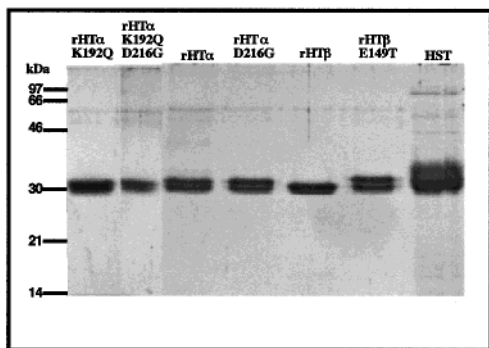


FIGURE 2: SDS-PAGE of purified rHTs and HST. Lanes 1 through 5 contain approximately 1 μ g of the indicated rHT. Lane 6 contains 3 μ g of HST.

Leu151 as the cleavage site; Arg150 is preceded by several negatively charged residues somewhat resembling the four consecutive Asp residues in the EKCS (see Figure 1A). Arg150 itself was not replaced because basic residues may be involved in heparin binding. A Pro at position 150 obviates the need for a similar mutation in rHT α .

Purification and Physical Properties. Partially purified fusion proteins derived from the expression rHTs were processed by treatment with EK as previously described (28). After treatment, a decrease in mass upon SDS-PAGE consistent with cleavage at the EKCS was observed for all rHTs except for rHT β , which revealed mature protease as well as further hydrolyzed products as discussed above. Liberated rHTs were purified as described in Experimental Procedures. In the final fractionation on heparin Sepharose, all rHTs eluted at 0.7 M NaCl.

Purified rHTs analyzed by SDS-PAGE demonstrated singlet or doublet band(s) migrating with an apparent mass of 30 kDa, consistent with the size of rHT subunits (Figure 2). The doublet banding pattern likely is due to variable glycosylation of two different sites. rHT α has two glycosylation sites, and a second glycosylation site was introduced into the rHT β variant when Glu149 was mutated to Thr (Figure 1A). Purified HST, also shown in Figure 2, appears as a more diffuse band of similar size to rHTs. The more distinct banding pattern of the rHTs likely reflects their less extensive glycosylation upon expression in insect cells.

Sedimentation equilibrium analyses of rHT α -D216G were performed under stabilizing conditions of 2 M NaCl, 0.01 M MOPS, pH 6.8. Plots of $\ln A_{280 \text{ nm}}$ vs radial position squared were linear at all concentrations and speeds, demonstrating a homogeneous population of protein species with an average mass of 106 ± 5 kDa ($n = 11$). This value is equivalent to that of 113 ± 13 kDa obtained by a similar analysis of stabilized HST tetramer (14). These masses are consistent with that expected for a tetramer composed of four subunits of 27.6 kDa.

Purified rHTs were analyzed by SEC under stabilizing conditions of 2.0 M NaCl, pH 6.8, 25 $^{\circ}$ C (Figure 3). All rHTs eluted as a single peak slightly after IgG (150 kDa). The elution profiles of rHT α and two variants, rHT α -D216G and rHT α -D216G-K192Q, are shown in Figure 3. Except for rHT α and rHT α -K192Q, hydrolysis of tosyl-GPK-NA was associated with these peaks. More than 95% of the activity applied to the column was recovered in the peak fractions. These results demonstrate further the purity of the rHT preparations and show that all are likely tetrameric.

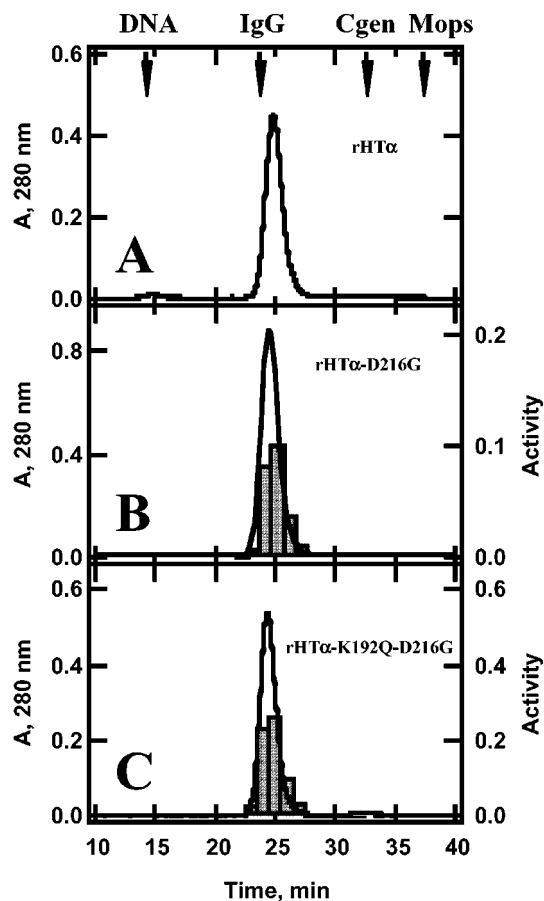


FIGURE 3: SEC analysis of purified rHT α s. rHT α s in panels A–C were chromatographed on a Superose 12HR 10/30 FPLC column under stabilizing conditions of 2.0 M NaCl, 0.01 M MOPS, pH 6.8. Proteases were loaded at a concentration of 1.0 mg/mL (40 μ M). $A_{280 \text{ nm}}$ was measured using a flow-cell, and hydrolytic activity was determined from collected fractions. Activity measured using 1 mM tosyl-GPK-NA is reported as $\Delta A_{410 \text{ nm}}/\text{min}/\text{aliquot of } 5 \mu\text{L}$, and is displayed as a histogram. Elution positions of DNA (void volume), IgG (150 kDa), chymotrypsinogen (23.5 kDa), and MOPS (total volume, monitored by $A_{230 \text{ nm}}$) are indicated by arrows.

The CD spectra of rHTs are compared to those of active and spontaneously inactivated HST in Figure 4. Spectra were obtained in 2 M NaCl, 0.01 M MOPS, pH 6.8. rHT α , rHT α -D216G, and rHT β -E149T all demonstrated a negative peak at 230 nm. This peak is a feature of the active form of HST and HLT and is not present in the spectra of either HT after spontaneous inactivation (14, 36). Consistent with CD, IFE spectra of rHT β , rHT β -E149T, rHT α , and rHT α variants were similar to each other and to that of active HST (11). The IFE maximum of active HST and rHTs was at 330 nm as compared to 334 nm for inactivated HST (11). The results of these spectroscopic studies indicate that rHT α , rHT β , and variants are folded similar to active HT isolated from tissues.

Catalytic Properties of rHTs. To test for catalytic ability, all rHTs were titrated with the burst titrant MUGB. rHT α and rHT α -K192Q showed no reaction. All other rHTs reacted rapidly with MUGB demonstrating a burst of activity consistent with the rHT concentration based on $A_{280 \text{ nm}}$.

The kinetic parameters of rHTs were evaluated using a series of model substrates commonly used to measure the hydrolytic activity of trypsin-like proteases, including HST. Reported in Table 1 are specific activities determined at 1 or 0.5 mM (tosyl-GPR-NA) substrate concentration, and $k_{\text{cat}}/$

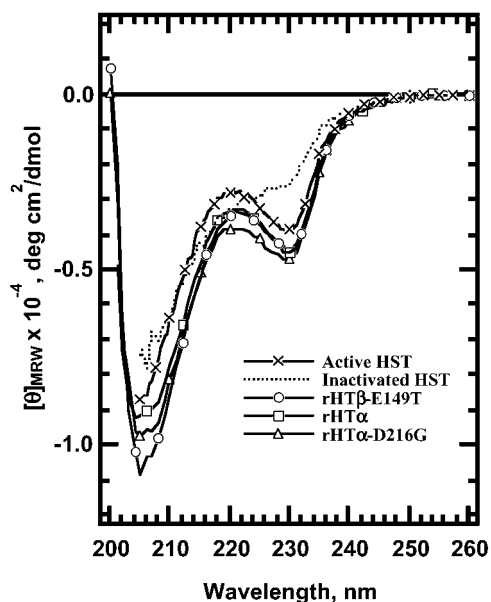


FIGURE 4: CD spectra of rHTs. Spectra were obtained under the stabilizing condition of 2 M NaCl, 0.01 M MOPS, pH 6.8, 25 °C. Previously reported spectra of active (230 nm peak) and spontaneously inactivated HST are included for comparison (14).

Table 1: Kinetic Parameters for the Hydrolysis of Model Substrates by HST and rHTs

tryptase ^a	substrate ^b	specific ^c activity	$10^{-3} \times k_{\text{cat}}/K_m^d$ $\text{M}^{-1} \text{s}^{-1}$
HST	L-BAPNA	0.21	2.2
	CBZ-GPR-NA	4.1	86
	tosyl-GPK-NA	3.2	46
rHT β	tosyl-GPR-NA	3.2	86
	L-BAPNA	0.14	3.0
	CBZ-GPR-NA	3.3	97
	tosyl-GPK-NA	2.7	53
rHT β -E149T	tosyl-GPR-NA	3.4	92
	L-BAPNA	0.16	2.9
	CBZ-GPR-NA	3.3	80
	tosyl-GPK-NA	2.3	37
rHT α -D216G	tosyl-GPR-NA	3.5	75
	L-BAPNA	0.0 ^e	0.0
	CBZ-GPR-NA	0.17	4.6
	tosyl-GPK-NA	0.22	4.4
rHT α -K192Q-D216G	tosyl-GPR-NA	0.20	11
	L-BAPNA	0.0	0.0
	CBZ-GPR-NA	1.0	25
	tosyl-GPK-NA	1.0	24
	tosyl-GPR-NA	1.4	45

^a Data for rHT α and rHT α -K192Q are not included because activity was not detected with the above substrates in 60-min incubations with high concentrations (4 μM) of enzyme and 1 mM substrate. ^b Assay conditions in all measurements were 0.2 M NaCl, 0.1 M Tris, pH 8.0, 9% DMSO, 0.1 mg/mL heparin, 25 °C + substrate. ^c For specific activity measurements $[\text{S}]_0 = 1 \text{ mM}$ except for tosyl-GPR-NA where $[\text{S}]_0 = 0.5 \text{ mM}$; HT concentrations ranged from 2 to 35 nM. The units for specific activity are ($\mu\text{mol of NA min}^{-1}$)/(nmol subunit). ^d For k_{cat}/K_m determinations, $[\text{S}]_0 = 0.05 \text{ mM}$; HT concentrations ranged from 0.01 to 0.7 μM . Values are the averages of 2–4 determinations and SDs were $\leq 10\%$ of the averages. ^e 0.0 indicates no detectable hydrolysis in assays monitored for 60 min with rHT α -D216G = 0.4 μM and rHT α -K192Q-D216G = 0.3 μM .

K_m values determined under pseudo first-order conditions with $[\text{S}]_0 \ll K_m$. Under our assay conditions, K_m and k_{cat} values could not be determined from initial velocity versus substrate concentration plots due to the limited solubility of the substrates (see Experimental Procedures). Plots were

either linear or only slightly curved over the attainable substrate concentration ranges. In view of these limits, we estimate that K_m values for all enzymes/substrates were greater than 0.8 mM.

Specific activities and k_{cat}/K_m values for the hydrolysis of substrates by rHT β and rHT β -E149T were similar to those for HST. The two rHT α variants that reacted with MUGB also catalyzed the hydrolysis of model peptide substrates. Catalytic efficiencies were lower than those of rHT β (s). rHT α -K192Q-D216G was a more efficient catalyst than rHT α -D216G. For the three peptide substrates, it exhibited k_{cat}/K_m values that were 5–40-fold greater than those of rHT α -D216G, and 2–4-fold less than those of the rHT β (s). Neither rHT α -K192Q-D216G nor rHT α -D216G catalyzed the hydrolysis of the single residue substrate L-BAPNA.

Purified preparations of rHT α and rHT α -K192Q did not produce detectable hydrolysis under conditions and enzyme concentrations used to assay HST and rHT β s. A small amount of catalytic activity was detected in both preparations using a more sensitive assay. The assay conditions were 1 h duration, 1 mM tosyl-GPK-NA (0.2 M NaCl, 0.1 M Tris, pH 8.0, 0.1 mg/mL heparin, 25 °C), and protease concentrations approximately 1000-fold higher than those used to measure rHT β activity. The activity measured corresponded to less than 0.05% of the activity for an equivalent concentration of rHT β and could be completely inhibited by a concentration of the irreversible inhibitor, AEBFSF, equivalent to less than 10% of the subunit concentration. Inhibition by a substoichiometric concentration of inhibitor therefore indicates that the source of the catalytic activity is likely a contaminating protease present in small quantities. The absence of detectable catalytic activity for rHT α or rHT α -K192Q is in agreement with their lack of reaction with the active site titrant MUGB.

The inactivity of rHT α was further investigated using the competitive inhibitor pAb which binds to the S1 pocket of trypsin-like proteases including HST (11, 37). Burial within the S1 pocket produces an increase in IFE and a blue shift in the emission maximum as shown in a previous study with HST (11). rHT β -E149T was found to bind pAb similar to HST, while rHT α exhibited no detectable interaction. The lack of interaction suggests that the S1 pocket of rHT α is not accessible to substrates.

Studies on the spontaneous inactivation of HST and HLT imply that the free monomeric form of HT is either inactive (9, 11, 14) or exhibits much less activity than a subunit of the active tetramer (5). Rapid dissociation of rHT α upon dilution from stock conditions (2.0 M NaCl, 0.01 M MOPS, pH 6.8, 4 °C) to assay conditions (0.2 M NaCl, 0.1 M Tris-HCl, pH 8.0, 25 °C) might explain the lack of activity. As will be shown in the next section, the tetramer form of rHT α is very stable and therefore would not be expected to dissociate under assay conditions.

These results demonstrate a dramatic difference in the catalytic properties of rHT α and rHT β . rHT β demonstrated enzymatic activity similar to that of HST, while rHT α appeared enzymatically silent. As underscored by analysis of the rHT α S1-subsite variants, the Asp/Gly difference at position 216 was more critical to catalysis than the Lys/Gln difference at position 192.

Spontaneous Inactivation/Structural Stability of rHT β s. As shown in Figure 5 and Table 2, the functional stabilities of

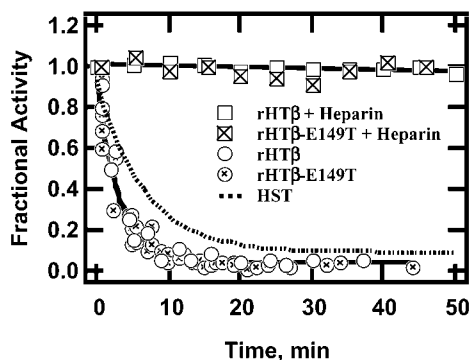


FIGURE 5: Spontaneous inactivation of rHT β and rHT β -E149T. Decay and control incubations were performed with 4 μ M rHT in 0.2 M NaCl, 0.01 M MOPS, pH 6.8, 30 $^{\circ}$ C with (boxes) and without (circles) 0.5 mg/mL heparin. Aliquots were removed at the indicated times and assayed for activity using L-BAPNA, as described in Experimental Procedures; remaining activity is reported as the fraction of activity present at time 0. The solid line through the decay data is a single exponential to the combined decays of rHT β and rHT β -E149T (half-life = 2 min, residual fractional activity = 0.04). For comparison, a similar fit is shown for the decay of 4 μ M HST (dotted line) under similar conditions; data were taken from Selwood et al. (11).

Table 2: Structural/Functional Stability of rHTs and HST

tryptase	half-life ^a , min				
	25 $^{\circ}$ C ^b		30 $^{\circ}$ C ^c		37 $^{\circ}$ C ^d
	A	A	F	A	F
HST	24	4.3	4.3	1.0	— ^e
rHT β	8.5	1.7	1.4	0.5	—
rHT β -E149T	7.5	2.3	1.5	1.0	—
rHT α	—	—	—	—	880
rHT α -K192Q	—	—	—	—	900
rHT α -D216G	—	385	—	85	82
rHT α -K192Q-D216G	35	14	—	1.8	—

^a Incubations were performed in 0.2 M NaCl, 10 mM MOPS, pH 6.8, at the indicated temperatures. Half-life values reported were calculated using rate constants obtained by fitting activity loss (columns marked A) or IFE decrease (columns marked F) data to a single-exponential function. HST data were taken from previous publications (6, 11, 14). ^b Values at 25 $^{\circ}$ C for rHTs were single determinations at rHT β = 5 μ M, rHT β -E149T = 4.0 μ M, and rHT α -K192Q-D216G = 0.5 μ M. ^c The values at 30 $^{\circ}$ C, column A, are the averages of multiple determinations made over a range of rHT concentrations. The concentration ranges (SD, number of determinations) were the following: rHT β = 0.15–3.5 μ M (0.3, n = 4), rHT β -E149T = 0.17–6.0 μ M (0.3, n = 9), rHT α -D216G = 0.4–4.0 μ M (72, n = 7), and rHT α -K192Q-D216G = 0.5–2.3 μ M (0.3, n = 4). As indicated by the small SDs, half-lives were independent of the rHT concentration. Values for rHTs in column F are from single determinations at rHT β = 0.5 μ M, rHT β -E149T = 0.4 μ M. ^d All values at 37 $^{\circ}$ C are from single determinations. Values in column A were determined at rHT concentrations identical to those used at 25 $^{\circ}$ C, rHT α -D216G = 1.0 μ M. The values in column F were obtained using rHT α and rHT α -K192Q = 0.3 μ M and rHT α -D216G = 1.0 μ M. ^e —, not determined.

rHT β and rHT β -E149T were characterized and compared to that of HST. Time-courses describing the inactivation of each rHT β at 4 μ M concentration are shown in Figure 5. Activity loss was somewhat faster and more complete than observed for HST (dashed line). The inactivation of rHT β and rHT β -E149T appeared indistinguishable. An exponential fit (solid line) to the combined data yielded a first-order rate constant of 0.032 min⁻¹ and a residual activity equivalent to 4% of the initial activity. The residual activity may reflect

Table 3: Rescue of Spontaneously Inactivated rHTs by Addition of Heparin

variant	[variant] μ M	inactivation ^a (- heparin)			after reactivation ^b (+ heparin)	
		$^{\circ}$ C	h	% initial activity	% initial activity	
rHT β	4.0	30	4.0	3	85	
	0.1	30	1.2	4	6	
rHT β -E149T	4.0	30	1.3	1	71	
	0.1	30	3.0	1	26	
rHT α -D216G	3.4	37	22.8	2	36	
rHT α -	2.3	30	1.9	4	62	
K192Q-D216G	1.2	30	18.6	4	42	
	0.4	37	0.7	2	2	

^a Conditions during inactivations were 0.2 M NaCl, 10 mM MOPS, pH 6.8, at the indicated temperatures. ^b After equilibration to 25 $^{\circ}$ C, reactivation was initiated by addition of 5 mg/mL stock heparin to the decay giving a final concentration of 0.5 mg/mL. Reactivations were monitored as a function of time until activity no longer increased (\approx 1 h).

an equilibrium between active and inactive forms of HT (11, 14).

Half-lives for activity loss of HST, rHT β , and rHT β -E149T at three temperatures are reported in Table 2 (columns marked A). Except for the somewhat faster activity loss of the rHT β s, all exhibit a similar temperature dependence. Activity was lost too rapidly to be measured precisely at 37 $^{\circ}$ C. Half-lives reported at 30 $^{\circ}$ C are the average of several decays obtained over a rHT concentration range of 0.15–6.0 μ M. As observed for HST, activity loss demonstrated little dependence on rHT concentration. SDs for the 30 $^{\circ}$ C data were less than 25% of the average values reported in Table 2. Spontaneous inactivation of HST is associated with a structural change as measured by a decrease in IFE (11). A similar IFE change was found for rHT β and rHT β -E149T (Table 2, column marked F). These results indicate that both rHT β and rHT β -E149T exhibit spontaneous inactivation similar to that observed for HST. The reason for the somewhat faster and the more complete loss of activity by the rHT β s relative to HST is unclear.

The effects of heparin on the spontaneous inactivation of rHT β s were similar to those observed with HST (11, 14). Low salt incubations containing heparin significantly reduced the rate of spontaneous inactivation (Figure 5). Addition of heparin to spontaneously inactivated rHT β s rescued up to 85% of the initial enzyme activity (Table 3) demonstrating the reversibility of the process. The extent of activity rescued on addition of heparin was dependent on the HT subunit concentration during the decay process (Table 3). The dramatic effects of heparin more completely establish the correspondence between rHT β , rHT β -E149T, and HST.

Spontaneous Inactivation/Structural Stability of rHT α s. Two of the four rHT α s analyzed, rHT α and rHT α -K192Q, did not catalyze the hydrolysis of model substrates. Spontaneous inactivation of HST (11) and rHT β (previous section) is accompanied by a change in their IFE spectra. As will be described below, spontaneous inactivation of rHT α -D216G demonstrated a similar IFE change, indicating that IFE can be used to assess structural change associated with the spontaneous inactivation of rHT α s with no detectable

catalytic activity. Also used to assess structural change was SEC which monitored tetramer stability.

In Figure 6A and B, time-courses monitoring IFE change and activity of rHT α -D216G incubated under decay conditions of 0.2 M NaCl, 0.01 M MOPS, pH 6.8, 37 °C (\pm 0.5 mg/mL heparin) are shown. In the absence of heparin, both IFE and activity decreased in an exponential manner. First-order rate constants calculated by fitting the data to an exponential function yielded similar values of 0.0085 ± 0.0005 and 0.0082 ± 0.0008 min⁻¹ for IFE and activity, respectively. The similar rate constants for the IFE and activity decreases of rHT α -D216G suggest that the same process is being monitored using both techniques as was observed previously for HST (11). Consistent with that observed for HST (6), HLT (5, 7), and rHT β s, the presence of heparin greatly reduced the rate of IFE and activity decrease. These results indicate that rHT α -D216G undergoes spontaneous inactivation similar to HST, although at a slower rate.

Using IFE, rHT α was monitored under the same decay and stabilizing conditions described for rHT α -D216G (Figure 6C). In contrast to rHT α -D216G, rHT α showed very little change in IFE over the 8-h incubation period used for rHT α -D216G. rHT α was equally stable in incubations performed at pH 6.8 and 8.0 demonstrating that the stability of rHT α was not due to the slightly lower than physiological pH routinely used in these studies. We have shown previously that the functional stability of HST is unaltered through the same pH range (6). Continued monitoring of rHT α over a 3-day period demonstrated a slow, exponential-appearing, decrease in IFE (Figure 6C). The slowness makes it unclear whether the decrease was due to a specific or nonspecific process. Parallel incubations in 0.01 M MOPS, pH 6.8, 37 °C containing 2 M NaCl or heparin (0.5 mg/mL) showed no decrease in IFE. These results suggest that rHT α is much more stable than rHT β and that Asp216 is a factor in determining rHT α stability.

The half-lives for spontaneous activity loss or IFE decrease for rHT α , rHT β , and S1-subsite variants of rHT α are compared in Table 2, and the rescue of inactivated rHTs by heparin are compared in Table 3. rHT α -K192Q, which was not enzymatically active, demonstrated a slow decrease in IFE similar to rHT α . In contrast, the double mutant, rHT α -D216G-K192Q, which was a better catalyst than rHT α -D216G, exhibited a rate of activity loss significantly faster than rHT α -D216G and close to that of rHT β . Consistent with the properties of spontaneous inactivation, rHT α variants exhibiting catalytic activity could be rescued by the addition of heparin after inactivation (Table 3).

The stability of rHT α relative to the least stable rHT α variant, D216G-K192Q, is further demonstrated by SEC in Figure 7. Even after 17 h of incubation under decay conditions, rHT α migrated largely as a tetramer (Figure 7A). The symmetrical appearance of the peak suggests little tendency to dissociate even upon dilution on the column. The concentration of rHT α loaded onto the column was 4 μ M as compared to 500 nM in the eluted tetramer peak. In contrast, a similar concentration of rHT α -D216G-K192Q was completely dissociated after a 1 h incubation under the same decay conditions (Figure 7B). Dissociated rHT α -D216G-K192Q and rHT α appeared to be monomeric eluting between α 1-antichymotrypsin, 45 kDa, and chymot-

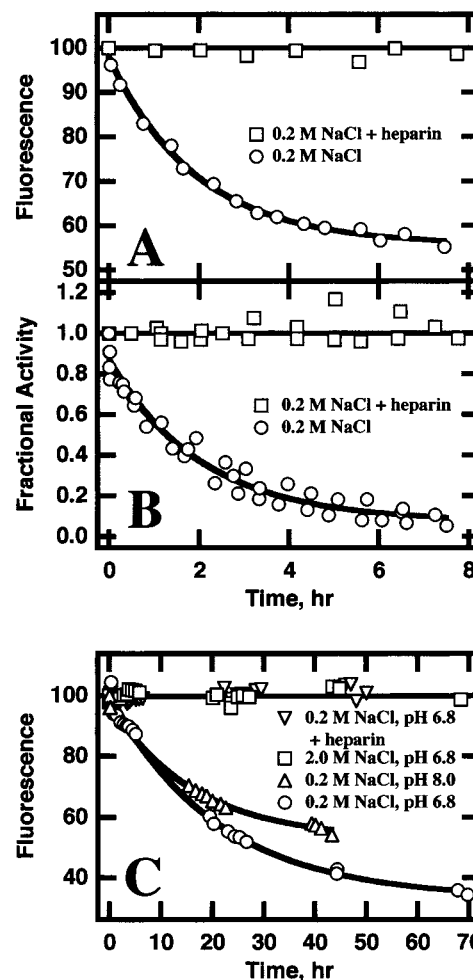


FIGURE 6: Time-courses of enzymatic activity and/or IFE change of rHT α and rHT α -D216G upon incubation at 37 °C. Shown in panel A are IFE (330 nm) changes associated with rHT α -D216G when incubated in 0.2 M NaCl, 0.01 M MOPS, pH 6.8, 1 μ M enzyme in the presence and absence of 0.5 mg/mL heparin. In panel B, are time-courses monitoring enzymatic activity of rHT α -D216G under the same conditions as panel A. Activity was measured using 1.0 mM tosyl-GPK-NA and converted to fractional activity, as described in Experimental Procedures. In panel C, the time-courses of IFE (330 nm) change of rHT α when incubated at 37 °C in the indicated conditions. The concentration of rHT α in all time-courses was 280 nM. Buffers were 0.01 M MOPS at pH 6.8 and 0.1 M Tris-HCl at pH 8.0. The concentration of heparin in the control was 0.5 mg/mL.

rypsinogen, 23.5 kDa. The IFE spectrum of inactive rHT α -D216G-K192Q demonstrated a maximum at 334 nm similar to inactivated HST (11).

These results demonstrate that rHT α is a more stable form of HT than rHT β , and that residues associated with the formation of the S1 pocket are largely responsible for this difference in stability. Similar to that observed for catalytic properties, the stability of rHT α was more dependent upon Asp216 than Lys192.

DISCUSSION

In the present study, rHTs with amino acid sequences corresponding to the HT α .I and HT β .II isoforms were produced recombinantly and characterized. While exhibiting similar gross structural and spectral features, they differed markedly in enzymatic activity and stability with respect to

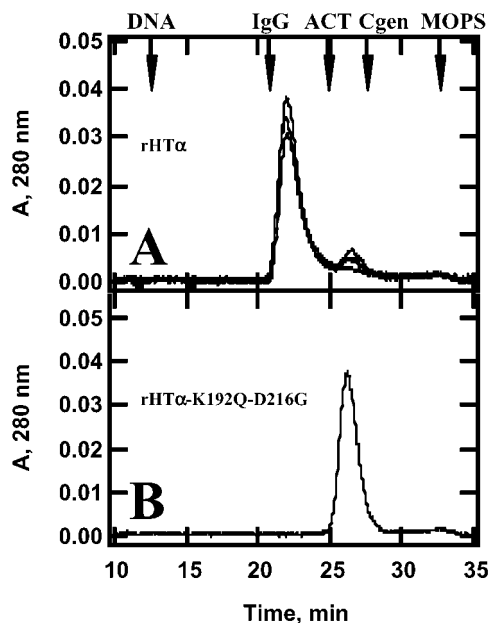


FIGURE 7: Change in quaternary structure of rHT α and rHT α -D216G-K192Q during spontaneous inactivation. rHT at 4 μ M concentration was incubated at 37 $^{\circ}$ C in 0.2 M NaCl, pH 6.8, 0.01 M MOPS. At various times, 250 μ L samples were analyzed by SEC at 25 $^{\circ}$ C in a column equilibrated with 0.2 M NaCl, and 0.01 M MOPS, pH 6.8. The three profiles obtained for rHT α (panel A) were obtained after 0, 1, and 17 h of incubation. A small progressive decrease in the tetramer peak is complemented by a small increase in the monomer peak. The profile for rHT α -K192Q-D216G (panel B) was obtained after 1 h incubation. Column and standards used for calibration are those described in Figure 3 except for α -1-antichymotrypsin (ACT, 45 kDa); arrows mark elution times.

spontaneous inactivation. rHT β displayed catalytic and stability properties similar to those reported for HST. In contrast, rHT α did not catalyze the hydrolysis of model substrates and did not exhibit the rapid structural changes associated with spontaneous inactivation including dissociation to monomers. The correspondence between the properties of rHT β and those of HST and HLT suggests that this isoform is the major HT isolated from human tissues. Consistent with this premise, the HLT crystallized was confirmed to be HT β .II by analysis of enzymatic digestion products (8). Additionally, the close agreement between the specific activities of rHT β and HST reported in Table 1 strongly indicates that substantial amounts of inactive HT isoforms are not present in tissue preparations. The implied absence of rHT α from HST preparations is consistent with evidence that HT α s are not stored in mast cell secretory granules (10).

Catalytic Properties of rHT α and rHT β . The difference in catalytic properties between rHT α and rHT β was related to residues forming the S1 subsite, the primary substrate specificity pocket. In trypsin-like serine proteases, including HT β , the S1 subsite is a deep cleft capable of binding the side chains of Arg and Lys residues. The subsite is primarily formed by residues 189–195, 213–220, and 225–228 (8, 38, 39). rHT α and rHT β differ at residues 192 and 216. Systematic substitution of the residues in rHT α (Lys192, Asp216) by those in rHT β (Gln192, Gly216) showed that the dramatic differences in catalytic as well as stability properties (see below) between the isoforms was primarily the result of Asp or Gly at residue 216. Mutation of Lys192

to Gln became a factor only after Asp216 was replaced by Gly.

Residue 216 is located at the entrance to the S1 pocket (40, 41) and is a Gly in most serine proteases closely related to HT. The absence of a side chain allows efficient access of the side chain of the P1-residue of a substrate to the interior of the S1 pocket. The major exceptions are the elastases where residue 216 is a Val. The isopropyl side chain of Val216 partially fills the S1 pocket, thereby limiting the specificity of elastases to substrates with small aliphatic residues at P1 (42, 43). Thus, dramatic effects on enzymatic activity due to the accessibility of the S1 subsite could occur by replacing Gly with another residue.

Large decreases in catalytic efficiency have been observed upon mutation of Gly216 of trypsin-like proteases. The natural mutation of Gly216Ser in protein C (44) and the engineered mutation of Gly216Ala in trypsin (40) reduced the catalytic efficiency of these proteases markedly. The effect of Ala216 on trypsin catalysis suggests that even a small side chain will have a dramatic effect. Given the similarity of the S1 subsite fold between trypsin and HLT (8), and the similarity of the physical properties between rHT α and rHT β described here, it is likely that the low activity of rHT α is due, at least in part, to the side chain of Asp216 filling S1 pocket and sterically blocking or altering the binding of the P1 residue of substrates.

Obstruction of the S1 pocket is consistent with the inability of rHT α to react with the active site titrant, MUGB, and the competitive inhibitor, pAb. We have shown that the S1 pocket of spontaneously inactivated HST does not react with MUGB and does not bind pAb (11). Because the spectral properties of rHT α corresponded to active and not inactivated HST, the inaccessibility of the S1 pocket is not related to rHT α adopting a conformation corresponding to the spontaneously inactivated state(s).

Consistent with the importance of the 216 position to substrate accessibility, rHT α -D216G exhibited readily detectable catalytic activity, while rHT α -K192Q was inactive like rHT α . However, rHT α -D216G catalytic efficiency was reduced as compared to that of HST/rHT β . Significant improvement in catalytic efficiency to a level near that of HST/rHT β was observed for rHT α -K192Q-D216G. Nevertheless, the double mutant still did not completely reproduce the catalytic efficiency of rHT β or HST with peptide substrates and neither active rHT α variant catalyzed the hydrolysis of the single-residue substrate L-BAPNA.

A previous study by Huang et al. (25) recognized a generally similar activity relationship between rHT α , rHT β , and rHT α -D216G. They found that rHT α was unable to efficiently hydrolyze substrates of rHT β , and that mutation of Asp216 to Gly significantly improved catalytic efficiency, but not to the level of rHT β . On the basis of the loop structures contributing to the formation of the substrate binding site of HT β , it was suggested that further differences at residues 37, 59, 192 and in the 97 loop might play a role in modulating the catalytic properties of HT α and HT β . Our studies could not demonstrate a role for residue 192 unless its mutation was coupled to mutation of residue 216. Eliminated by our study is a role for residue 59, as our rHT α construct contained the rHT β residue Val at this position (see Figure 1). We speculate that the inability of our double mutant rHT α -K192Q-D216G to completely reproduce the

activity of HT β could be due to the three residue difference in the 97 loop (Figure 1). In rHT β , this loop appears to have a complex role. The 97 loop helps to form one of the interfaces producing the rHT β tetramer, thereby complicating its more usual role of contributing to the structure of the S2 and S4 subsites (8).

Huang et al. (25) showed that rHT α could be labeled with radioactive DFP, indicating that the catalytic machinery of the protease (Ser195–His57–Asp102 catalytic triad) was functional. Surveying a large number of substrates including fibrinogen, they reported hydrolysis of only two substrates, tosyl-GPK-NA and H-D-HHT-AR-NA. Activity was very low, described as positive activity after a 4-h incubation at 15 nM rHT α in 0.075 mM substrate, pH 7.4. Given these findings and noting the presence of Asp189 at the bottom of the S1 pocket, Huang et al. (25) suggested that rHT α is a trypsin-like protease with a highly limited substrate specificity. Unlike Huang et al. (25), we found that rHT α did not hydrolyze model substrates with Arg or Lys at the P1 position or react with the active site titrant MUGB. Included among the substrates tested in our study was tosyl-GPK-NA. In a 60-min assay containing 4 μ M rHT α and 1 mM substrate, pH 8.0, virtually no product formation was observed over that produced by a low level of a contaminating protease inhibited by a substoichiometric (0.4 μ M) concentration of inhibitor. The reasons for the different results are unclear; nevertheless, taken together both studies strongly suggest that rHT α is not a highly efficient trypsin-like protease. The inability of rHT α to recognize “efficiently” substrates with Lys or Arg at the P1 position is consistent with an inaccessible S1 subsite.

Another difference between the two studies is related to the hydrolysis of L-BAPNA by rHT β . Huang et al. (25) reported that rHT β was unable to turnover this substrate. We find that rHT β catalyzed the hydrolysis of L-BAPNA with similar efficiency to HST. This is important because rHT α -D216G and rHT α -K192Q–D216G did not catalyze the hydrolysis of L-BAPNA. Thus, the absence of L-BAPNA hydrolysis is likely a property reflective of the unusual active site structure of rHT α in addition to Lys192 and Asp216.

Stability Properties of rHT α and β . Mutations to the S1 subsite that increased the catalytic efficiency (k_{cat}/K_m) of rHT α also decreased its stability as measured by the rate of spontaneous inactivation and/or IFE decrease. Under conditions where rHT β lost activity with a half-life of roughly 1 min (Table 2, 37 °C), rHT α exhibited only a slow decrease in IFE ($t_{1/2} = 900$ min). In contrast, rHT α -D216G inactivated much more rapidly ($t_{1/2} = 68$ min) and by a process with the characteristics of spontaneous inactivation. However, the rate of activity loss was still approximately 100-fold slower than that observed for rHT β . The double mutant, rHT α -K192Q–D216G, which demonstrated catalytic efficiency close to that of rHT β , exhibited a rate of activity loss only 2–5-fold slower than rHT β . As was the case for catalysis, the residue at 216 underpins the stability of rHT α since the single mutant rHT α -K192Q displayed stability and catalytic properties similar to rHT α .

The relationship between activity and functional stability suggests that as rHT α becomes more competent for catalysis its stability decreases. The central role of Asp216 may be reconciled if the Asp216 side chain not only blocks the S1 pocket decreasing catalytic efficiency, but at the same time

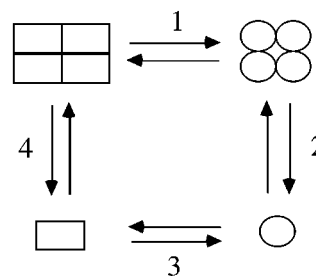


FIGURE 8: Minimal pathways for HT spontaneous inactivation and associated tetramer dissociation. Rectangles denote active HT subunits, and circles indicate inactive HT subunits. In pathway one, inactivation is produced by a conformational change in each subunit of the tetramer (step 1). The result is an inactive-destabilized tetramer in equilibrium with monomer (step 2). In the second pathway, dissociation of the active tetramer (step 4) occurs prior to an inactivating conformational change (step 3).

stabilizes the site against spontaneous inactivation. We have shown that spontaneously inactivated HST no longer binds pAb, indicating that the structure of the S1 pocket is disrupted during spontaneous inactivation (11). Correspondingly, competitive inhibitors, such as leupeptin and pAb, that bind to the S1 subsite markedly stabilize the protease as monitored by physical methods (11, 14). The normal structure of the S1 pocket in the HLT crystal structure was likely due to the presence of the inhibitor, APPA (8).

How an Asp at position 216 could produce a more stable S1 pocket is not yet clear. The bottom of the S1 pocket in HT is negatively charged, such that the anionic side chain of Asp216 might have been expected to destabilize the region. A potential ionic bond with Lys192 was considered; however, the stability of rHT α -K192Q seems to argue against such a bond. Perhaps hydrogen bonding between the carboxyl group of Asp216 and other residues mediated by buried solvent molecules is the stabilizing factor.

Mechanism of Spontaneous Inactivation. A minimal scheme for HT spontaneous inactivation involving a conformational change and tetramer dissociation is shown in Figure 8. We have proposed that spontaneous inactivation is the relaxation of the active enzyme to a zymogen-like conformation (11, 14), i.e., a conformation with the S1 subsite, oxyanion hole, and the Ile16–Asp194 salt bridge disrupted (15). On the basis of sedimentation equilibrium analyses of active and inactivated HST we suggested that step 1 is the primary pathway for salt-bridge disruption and that dissociation (step 2) is a consequence of tetramer destabilization related to this structural change (14). Alternatively, it has been suggested that spontaneous inactivation is due to the instability of monomers (step 3), and that dissociation of the active tetramer (step 4) initiates the process (12, 13, 16). Underlying the latter model is the assumption of a weak tetramer structure that readily dissociates in the absence of heparin.

The stability of the rHT α tetramer described in this study further supports our position that dissociation of the active tetramer does not initiate spontaneous inactivation. rHT α demonstrated little tendency to dissociate when incubated under physiological conditions for up to 17 h (Figure 7), suggesting that intersubunit contacts forming the tetramer are not inherently weak. These contacts should not have been altered in the variant, rHT α -K192Q–D216G, a S1-subsite variant of rHT α that demonstrated functional instability

similar to rHT β and subunit dissociation after 1 h of incubation under physiological conditions. The similar stability properties of rHT α -K192Q-D216G and rHT β eliminates the possibility that residue differences within interface regions of HT α and HT β have a role in spontaneous inactivation. The corresponding small and large interfaces of rHT α and rHT β each differ by four residues. Included among the interface differences is an Arg for a Pro at position 150. Arg150 is located at the small interface of the HT β .II tetramer (8); the close proximity of the guanidyl groups of Arg150 in opposing subunits seen in the crystal structure was proposed as a factor underlying tetramer instability/spontaneous inactivation (13, 16). Also eliminated as a factor is the 37 loop which differs by three residues in rHT α -K192Q-D216G and rHT β .

The unusual frame-like structure of the HT tetramer, the small size and asymmetry of one of the subunit interfaces, and the proximity of both interfaces to the S1 pocket certainly provide a rationale by which structural change at the S1 pocket could be transmitted to loops forming the two subunit interfaces. As noted from the crystal structure, this link might be the Ile16-Asp194 salt bridge (13, 16). It was suggested that adjacent regions/residues capable of electrostatic interaction with the charged groups of Ile16 and Asp194 might make this bond unusually weak (13, 16). Of most interest was the charge and position of the 147 loop of the small interface. This loop contains several anionic residues (Asp143, Asp145, Asp147, and Glu149) and is located adjacent to Val17-Gly19. An alternative site that could neutralize Asp194 was suggested to be His40 which stabilizes Asp194 in trypsinogen and probably in proHT.

In the context of our model of spontaneous inactivation, decay conditions would favor the alternative binding of the salt bridge components to His40 and the 147 loop (step 1, Figure 8). HT in this configuration would be the predicted destabilized tetramer. A critical role for His40 and the negatively charged residues in the 147 loop remains to be explored. The negative charge of the 147 loop in our fusion protein was recognized by EK and was the reason for construction of the variant, rHT β -E149T. The similar properties of rHT β and rHT β -E149T appear to rule out an individual role for Glu149 in spontaneous inactivation.

Binding of heparin greatly slows spontaneous inactivation and rescues spontaneously inactivated HT. The dependence of HT stability on heparin chain length has been interpreted to suggest that bound heparin spans across subunits and stabilizes the tetramer in a clamp-like manner (1, 12, 13, 16). If intersubunit contacts in the active conformation are relatively stable, then heparin binding must stabilize HT in some other manner. In our model, heparin binding would serve to stabilize the S1 subsite in the active conformation (step 1). This effect may be accomplished by a strengthening of the Ile16-Asp194 bond. The Ile16-Asp194 bond is in the vicinity of the small interface, and a model of heparin bound to the HT tetramer shows the glycosaminoglycan spanning this interface (13).

The results reported in this study as well as those on rHT catalysis reported by Huang et al. (25) suggest that HT α and HT β isoforms differ markedly in catalytic ability and stability, and that the identity of the 216 residue as Gly or Asp is the primary factor determining the properties of the gene products. The side chain of Asp216 most likely extends

into the S1 pocket blocking the entry of substrates while stabilizing the tetrameric structure perhaps through interactions with surrounding structure. The conversion of rHT α to a rHT β -like HT by mutation of residues in the S1 subsite, most importantly Asp216, suggests that upon spontaneous inactivation tetramer dissociation occurs subordinate to or coordinate with a conformational change at the S1 pocket. A link between conformational change at the S1 pocket and the small subunit interface may be the disruption of the Ile16-Asp194 salt-bridge. The stabilizing role of heparin on HT function may be to strengthen this salt-bridge.

ACKNOWLEDGMENT

Special thanks to Michael Plotnick for helpful discussions and to Jason Andres and Holly Smolensky for technical assistance. rHTs were expressed at the Expression Vector Recombinant Protein Facility located at the Wistar Institute. CD and analytical ultracentrifugation studies were performed at the Biophysics Instrumentation Facility, University of Wisconsin, which was established by funding from the University of Wisconsin and NSF Grant BIR-9512577.

REFERENCES

- Schwartz, L. B. (1994) *Methods Enzymol.* 244, 88-100.
- Smith, T. J., Houghland, M. W., and Johnson, D. A. (1984) *J. Biol. Chem.* 259, 11046-11051.
- Schwartz, L. B., Lewis, R. A., and Austen, K. F. (1981) *J. Biol. Chem.* 256, 11939-11943.
- Harvima, I. T., Schechter, N. M., Harvima, R. J., and Fräki, J. E. (1988) *Biochim. Biophys. Acta* 957, 71-80.
- Addington, A. K., and Johnson, D. A. (1996) *Biochemistry* 35, 13511-13518.
- Schechter, N. M., Eng, G. Y., and McCaslin, D. R. (1993) *Biochemistry* 32, 2617-2625.
- Schwartz, L. B., and Bradford, T. R. (1986) *J. Biol. Chem.* 261, 7372-7379.
- Pereira, P. J. B., Bergner, A., Macedo-Ribeiro, S., Huber, R., Matschiner, G., Fritz, H., Sommerhoff, C. P., and Bode, W. (1998) *Nature* 392, 306-311.
- Ren, S., Sakai, K., and Schwartz, L. B. (1998) *J. Immunol.* 1998, 4561-4569.
- Sakai, K., Ren, S., and Schwartz, L. B. (1996) *J. Clin. Invest.* 97, 988-995.
- Selwood, T., McCaslin, D. R., and Schechter, N. M. (1998) *Biochemistry*, 13174-13183.
- Kozik, A., Potempa, J., and Travis, J. (1998) *Biochim. Biophys. Acta* 1385, 139-148.
- Sommerhoff, C. P., Bode, W., Pereira, P. J., Stubbs, M. T., Sturzebecher, J., Piechotka, G. P., Matschiner, G., and Bergner, A. (1999) *Proc. Natl. Acad. Sci. U.S.A.* 96, 10984-10991.
- Schechter, N. M., Eng, G. Y., Selwood, T., and McCaslin, D. R. (1995) *Biochemistry* 34, 10628-10638.
- Stroud, R. M., Kossiakoff, A. A., and Chambers, J. L. (1977) *Annu. Rev. Biophys. Bioeng.* 6, 177-193.
- Sommerhoff, C. P., Bode, W., Matschiner, G., Bergner, A., and Fritz, H. (2000) *Biochim. Biophys. Acta* 1477, 75-89.
- Huang, R., Åbrink, M., Globl, A. E., Nilsson, G., Aveskogh, M., Larsson, G., Nilsson, K., and Hellman, L. (1993) *Scand. J. Immunol.* 38, 359-367.
- Miller, J. S., Westin, E. H., and Schwartz, L. B. (1989) *J. Clin. Invest.* 84, 1188-1195.
- Pallaoro, M., Fejzo, M. S., Shayesteh, L., Blount, J. L., and Caughey, G. H. (1999) *J. Biol. Chem.* 274, 3355-3362.
- Miller, J. S., Westin, E. H., and Schwartz, L. B. (1990) *J. Clin. Invest.* 86, 864-870.
- Vanderslice, P., Ballinger, S. M., Tam, E. K., Golstein, S. M., Craik, C. S., and Caughey, G. H. (1990) *Proc. Natl. Acad. Sci. U.S.A.* 87, 3811-3815.

22. Wong, G. W., Tang, Y., Feyfant, E., Sali, A., Li, L., Li, Y., Huang, C., Friend, D. S., Krilis, S. A., and Stevens, R. L. (1999) *J. Biol. Chem.* **274**, 30784–30793.
23. Caughey, G. H., Raymond, W. W., Blount, J. L., W.-T., H. L., Pallaoro, M., Wolters, P. J., and Verghese, G. M. (2000) *J. Immunol.* **164**, 6566–6575.
24. Chan, H., Elrod, K. C., Numerof, R. P., Sideris, S., and Clark, J. M. (1999) *Protein Express. Purif.* **15**, 251–257.
25. Huang, C., Li, L., Krilis, S. A., Chanasyk, K., Tang, Y., Li, Z., Hunt, J. E., and Stevens, R. L. (1999) *J. Biol. Chem.* **274**, 19670–19676.
26. Niles, A., Maffitt, M., Haak-Frendscho, M., Wheelless, C. J., and Johnson, D. A. (1998) *Biotechnol. Appl. Biochem.* **28**, 125–131.
27. Sakai, K., Long, S. D., Dove Pettit, D. A., Cabral, G. A., and Schwartz, L. B. (1996) *Protein Expr. Purif.* **7**, 67–73.
28. Wang, Z.-M., Walter, M., Selwood, T., Rubin, H., and Schechter, N. M. (1998) *Biol. Chem.* **379**, 167–174.
29. Mirza, H., Schmidt, V. A., Derian, C. K., Jesty, J., and Bahou, W. F. (1997) *Blood* **90**, 3914–3922.
30. Wang, Z.-M., Rubin, H., and Schechter, N. M. (1995) *Biol. Chem. Hoppe-Seyler* **376**, 681–684.
31. Horton, R. M., Hunt, H. D., Ho, S. N., Pullen, J. K., and Pease, L. R. (1989) *Gene* **77**, 61–68.
32. Ho, S. N., Hunt, R. D., Horton, R. M., Pullen, J. K., and Pease, L. R. (1989) *Gene* **77**, 51–59.
33. Pace, N. C., Vajdos, F., Fee, L., Grimsley, G., and Gray, T. (1995) *Protein Sci.* **4**, 2411–2423.
34. Jameson, G. W., Roberts, D. V., Adams, R. W., Kyle, W. S. A., and Elmore, D. T. (1973) *Biochem. J.* **131**, 107–117.
35. Laemmli, U. K. (1970) *Nature* **227**, 680–685.
36. Schwartz, L. B., Bradford, T. R., Douglas, C. L., and Chlebowski, J. F. (1990) *J. Biol. Chem.* **144**, 2304–2311.
37. Evans, S. A., Olson, S. T., and Shore, J. D. (1982) *J. Biol. Chem.* **257**, 3014–3017.
38. Bode, W. (1979) *J. Mol. Biol.* **127**, 357–374.
39. Perona, J. J., Hedstrom, L., Rutter, W. J., and Fletterick, R. J. (1995) *Biochemistry* **34**, 1489–1499.
40. Craik, C. S., Largman, C., Fletcher, T., Rocznik, S., Barr, P. J., Fletterick, R., and Rutter, W. J. (1985) *Science* **228**, 291–297.
41. Polgar, L. (1989) *Mechanism of Protease Action*, CRC Press, Boca Raton, FL.
42. Bode, W., Meyer, E., and Powers, J. C. (1988) *Biochemistry* **28**, 1951–1963.
43. Sinha, S., Watorek, W., Karr, S., Giles, J., Bode, W., and Travis, J. (1987) *Proc. Natl. Acad. Sci. U.S.A.* **84**, 2228–2232.
44. Marchetti, G., Patracchini, P., Gemmati, D., Castaman, G., Rodeghiero, F., Wacey, A., Cooper, D. N., Tuddenham, E. G. D., and Bernardi, F. (1993) *Br. J. Haematol.* **84**, 285–289.

BI015662V